Available online at www.sciencedirect.com
ScienceDirect
Biochimica et Biophysica Acta 1767 (2007) 441–448
Biochimica et Biophysica Acta
BBA
www.elsevier.com/locate/bbabio

Review

Correlation of electron transfer rate in photosynthetic reaction centers with intraprotein dielectric properties

Sergey K. Chamorovsky [a], Dmitry A. Cherepanov [b], Constantin S. Chamorovsky [c], Alexey Yu. Semenov [c,*]

[a] *Biological Faculty, Moscow State University, 119992 Moscow, Russia*
[b] *A.N. Frumkin Institute of Physical Chemistry and Electrochemistry, Russian Academy of Sciences, 117071 Moscow, Russia*
[c] *A.N. Belozersky Institute of Physical–Chemical Biology, Moscow State University, 119992 Moscow, Russia*

Received 28 September 2006; received in revised form 24 December 2006; accepted 15 January 2007
Available online 23 January 2007

Abstract

A number of the electrogenic reactions in photosystem I, photosystem II, and bacterial reaction centers (RC) were comparatively analyzed, and the variation of the dielectric permittivity (ε) in the vicinity of electron carriers along the membrane normal was calculated. The value of ε was minimal at the core of the complexes and gradually increased towards the periphery. We found that the rate of electron transfer (ET) correlated with the value of the dielectric permittivity: the fastest primary ET reactions occur in the low-polarity core of the complexes within the picosecond time range, whereas slower secondary reactions take place at the high-polarity periphery of the complexes within micro- to millisecond time range. The observed correlation was quantitatively interpreted in the framework of the Marcus theory. We calculated the reorganization energy of ET carriers using their van der Waals volumes and experimentally determined ε values. The electronic coupling was calculated by the empirical Moser–Dutton rule for the distance-dependent electron tunneling rate in nonadiabatic ET reactions. We concluded that the local dielectric permittivity inferred from the electrometric measurements could be quantitatively used to estimate the rate constant of ET reactions in membrane proteins with resolved atomic structure with the accuracy of less than one order of magnitude.

Keywords: Photosynthetic reaction center; Dielectric permittivity; Photoelectric activity; Rate constant; Marcus theory

1. Introduction

The processes of charge separation in photosynthetic reaction centers (RC) and further transfer of electron and proton along the photosynthetic chain are accompanied by generation of transmembrane electric potential difference ($\Delta\psi$) that can be detected using instrumental methods. The direct electrometric method suggested in our laboratory at the Belozersky Institute of Physical–Chemical Biology provided an opportunity to detect the rise-time of $\Delta\psi$ within the range from 200 ns to 100 ms [1–3]. This method was used to study bacteriorhodopsin [2], bacterial photosynthetic RC [3], as well as photosystem (PS) I [4,5] and PS II [6] of cyanobacteria.

Because the photoelectric signal amplitude measured by this method is proportional to dielectrically weighted distances, comparison of projections of the distance vectors between redox cofactors onto the membrane normal with the relative photovoltage amplitudes allows the local effective (i.e., determined within the reaction time interval) dielectric constant value (ε) to be estimated at the corresponding chain segment. Dielectric properties have a great influence on the mechanism of photoinduced electron transfer reactions in photosynthetic complexes, and their studies could provide a deeper advance in quantitative treatment of charge transfer reactions in membrane proteins. RCs seem to be an ideal object for such study because their 3D structure has been resolved with atomic resolution using X-ray diffraction analysis, and electron transport activity can be tested by various instrumental methods including laser spectroscopy, EPR, ENDOR, photoelectric techniques, etc. Photoelectric and

* Corresponding author. Tel./fax: +7 495 939 31 81.
E-mail address: semenov@genebee.msu.ru (A.Yu. Semenov).

0005-2728/$ - see front matter © 2007 Elsevier B.V. All rights reserved.
doi:10.1016/j.bbabio.2007.01.008

dielectric properties of RCs were considered in our earlier works [7–10]. The results of the studies are briefly summarized in Fig. 1. It follows from Fig. 1 that the value of ε is minimal at the core of the three complexes and gradually increases towards the periphery.

2. Dielectric and photoelectric properties of photosynthetic reaction centers

2.1. Photosystem I

Photoelectric and dielectric properties of PS I were studied using isolated PS I complexes and such complexes interacting with natural and artificial electron donors and acceptors. The results of X-ray diffraction analysis of crystals of the protein complex of photosynthetic RC were taken from the Brookhaven Protein Databank (http://www.rcsb.org/pdb). Distances between centers of molecules were measured using the HyperChem 7 Professional software.

The PS I electron transport chain includes P700 (special pair of chlorophyll (Chl) molecules), A_0 (one or the two Chl monomer molecules), A_1 (one or the two molecules of phylloquinone), and $[FeS]_4$ iron–sulfur clusters F_X, F_A, and F_B. Taking into account the distances between the PS I cofactors [11] and the structural model of the plastocyanin (Pc) docking site [12,13], as well as relative contributions of the electron transfer reactions P700 → A_0, A_0 → A_1 [14], A_1 → F_X [15, 16], F_X → F_B [17], Pc → P700 [18], and F_B → Fld (flavodoxin) [19]

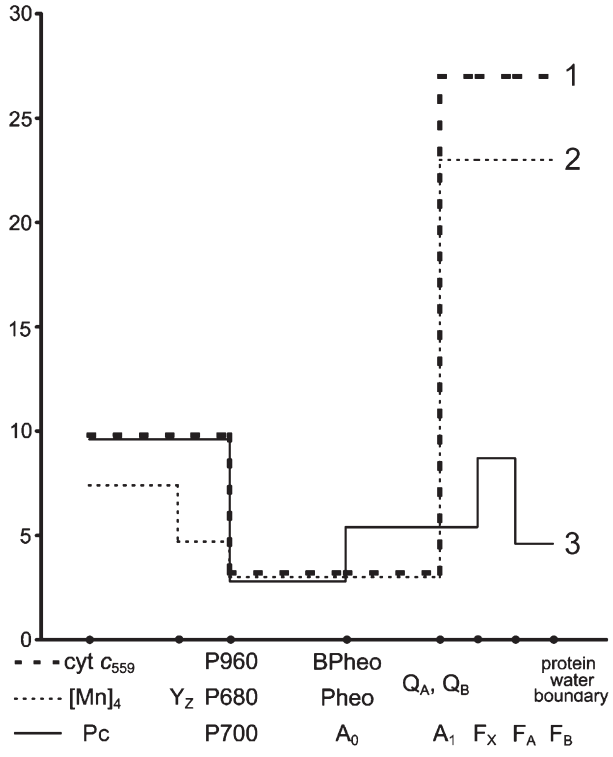

Fig. 1. Profile of changes of the effective dielectric constant ε along the photosynthetic RC complex: (1) RC of *Blastochloris viridis*; (2) photosystem II; (3) photosystem I.

to the overall electrogenesis provided by PS I complex, the following assertions were made:

(1) Let the minimal value of the dielectric constant for the P700 → A_0 protein region be ε ~ 3. Then, the ε value for the A_0 → A_1 and A_1 → F_X domains was estimated to be ~ 5.4.
(2) On the acceptor side, the ε value further increases nonmonotonically along the PsaC subunit (F_X → F_A, ε ~ 8.7; F_A → F_B, ε ~ 4.8).
(3) On the donor side between the Pc binding site and P700 Mg-porphyrin rings embedded into the PsaA/PsaB heterodimer (Pc → P700), the mean ε value is 9.7.

The estimates of ε are qualitatively consistent with the pattern of distribution of water molecules and ionizable amino acid residues (Asp, Glu, Lys, Arg, and His) in the loci of the electron transfer chain (Table 1). The numbers of ionizable amino acid residues in the vicinity of the iron–sulfur clusters F_X, F_A, and F_B (at distances < 11 Å from each cluster), determined from the X-ray diffraction analysis of the PS I protein crystals, are 13, 15, and 3, respectively. With regard to the effect of compensation of closely located opposite charges (distance, < 3.5 Å) [20], these numbers are 5, 9, and 3, respectively. Although the general trend towards an increase in the value of ε along the direction from the primary pair to the periphery of the complex is valid in this case too, there is a deviation from this trend at the site F_A → F_B, where distribution of water molecules and polar amino acid residues is abnormal. The cause of the anomaly is presently obscure.

2.2. Photosystem II

Recently determined crystal structures of PS II core complex from the cyanobacteria *Synechococcus elongatus* and *Thermosynechoccus vulcanus* [21–24] were resolved at 3.8 Å, 3.7 Å, and 3.0 Å resolution. It follows from these data that the arrangement of the electron transfer cofactors in PS II is rather similar to that in RCs of purple bacteria. The cofactors form two branches organized symmetrically along the pseudo-C2 axis. This symmetry is broken at the lumenal side of D1 protein by the redox-active Tyr 161 (Y_Z) and the manganese cluster $[Mn]_4$, which is located ~ 15 Å off the pseudo-C2 axis.

The kinetics and the quantum yield of the primary charge separation in pea chloroplasts were studied using the light-gradient technique [25,26]. The charge separation in PS II occurs with two electrogenic phases: the faster phase with the rise-time < 50 ps being ascribed to the electron transfer from the primary donor Chl dimer P680 to the intermediary acceptor pheophytin (Pheo), whereas the slower phase (~ 500 ps) being attributed to the electron transfer from Pheo to the primary quinone acceptor Q_A. The relative photovoltage contributions of the faster and slower phases were approximately equal to each other.

Fast photovoltage measurements using PS II membranes electrically oriented in a microcoaxial cell [27] and using PS II-containing proteoliposomes attached to a planar phospholipid

Table 1
Distances d from iron–sulfur centers to closest polar amino acid residues and water molecules in PS I complexes

Iron–sulfur centers	Amino acid residues												Water		
	ASP (−)		GLU (−)		LYS (+)		ARG (+)		HIS (+ at pH=6.0)		Total $d<11$ Å	Total $d<11$ Å with regard to compensation	No.	d (Å)	Total
	No.	d (Å)	No.	d (Å)	No.	d (Å)	No.	d (Å)	No.	d (Å)					
F_X	575	6.6	54[b]	10.8	51[b]	9.0	728[d]	5.1			**13**	**5**	162	4.2	**20**
	579[a]	8.3	62[a]	14.2			712[c]	5.6					43	5.3	
	566[b]	8.6					694	9.4					12	5.3	
	593[d]	8.6					674	9.6					190	6.0	
	580[c]	9.2					583[a]	9.7					73	6.3	
	568[a]	14.2					570[b]	10.5					37	6.4	
							65[b]	11.2					67	6.4	
							52[a]	12.0					6	6.6	
													26	6.9	
													145	7.0	
													36	7.0	
													56	7.4	
													132	8.1	
													64	8.3	
													76	8.4	
													160	8.4	
													159	8.5	
													188	8.7	
													158	8.9	
													157	9.2	
F_A	579[a]	7.3	4[b]	7.3	51[b]	8.4	583[a]	6.9	2	7.0	**15**	**9**	167	6.5	**11**
	23	8.3	62[a]	8.1	5	8.9	52[a]	7.7					25	6.6	
	46[e]	9.6	45	10.7			60	9.6					6.6	6.8	
	568[a]	11.3	71	10.7			43	9.9					145	6.8	
	566[b]	11.4					65[b]	10.2					76	8.0	
							570[b]	12.0					89	8.4	
							74[e]	12.6					165	8.4	
													166	8.6	
													34	8.8	
													119	9.4	
													120	10.4	
F_B	8	10.4	54[b]	10.1	51[b]	13.2	18	9.4			**3**	**3**	182	6.9	**8**
	566[b]	13.4					65[b]	11.4					126	7.1	
							570[b]	11.7					183	7.6	
													82	7.8	
													184	9.0	
													81	9.5	
													167	10.0	
													148	10.6	

The structure file was taken from RCSB Protein Data Bank, PDB ID: 1JB0 [11]. Distance measurements were performed using VMD 1.7.1 software (Theoretical Biophysics Group, Beckman Institute for Advanced Science and Technology, University of Illinois).

Distance d from amino acid residue to iron–sulfur center was measured as the shortest distance between the charged residue and the closest iron atom of the center. Groups of residues compensating each other are denoted as: a: ASP 579, ASP 568, GLU 62, ARG 583, ARG 52; net charge −1; b: ASP 566, GLU 54, LYS 51, ARG 570, ARG 65; net charge +1; c: ASP 580, ARG 712; net charge 0; d: ASP 593, ARG 728; net charge 0; e: ASP 46, ARG 74; net charge 0.

membrane [6,28] showed that electron transfer from Y_Z to $P680^+$ spanned a dielectrically weighted distance of 13–18% of the distance between P680 and Q_A. The dielectrically weighted distance of the electron transfer from $[Mn]_4$ to Y_Z^{ox} ($S_1 \rightarrow S_2$ state transition of the oxygen-evolving complex) was estimated to be less than 3.5% [28, 29]. Larger electrogenic components (about 7%) were attributed to proton transfer from the oxidized cofactor X to the lumen phase during the transition $S_2 \rightarrow S_3$ [28].

As it was shown earlier, the charge transfer reaction associated with protonation of double-reduced secondary plastoquinone Q_B^{2-} at the acceptor side contributes about 5% to the overall electrogenesis in PS II [30,31]. However, this estimate represented the lower limit of the relative contribution of this reaction, because: (i) the reconstruction of the Q_B function in the PS II particles used in these experiments was incomplete and (ii) slow component of $\Delta\psi$ decay (characteristic of the oxygen-evolving complex activity [32]) contributed only ~50% to the overall laser flash-induced $\Delta\psi$ decay [30]. It was shown recently in our laboratory using PS II preparations, in which the contribution of the slow component of the $\Delta\psi$ decay reached ~90%, that the amplitude of the electrogenic phase attributed to Q_B^{2-} protonation was ~11% of the total amplitude of $\Delta\psi$ [33]. The distance between the Q_B-binding site and protein globule boundary in PS II complexes is smaller than in bacterial RC [24]. Therefore, it is safe to suggest that the dielectric properties in the Q_B-protein boundary domain of PS II are similar to that of bacterial RC.

Like in the case of the bacterial RC, the ε value in the protein domain between the Chl dimer P680 and Q_A is the lowest, whereas it gradually increases at the donor side. A similar (but less significant) increase in the effective dielectric constant is observed at the donor side of PS II.

2.3. Bacterial reaction centers

Although the PS I complex differs significantly from the RC of purple photosynthetic bacteria, there are features of remarkable similarity between PS I and bacterial RC, especially in the RC core and the donor sites. It was shown in our earlier studies that electrogenic reduction of the photo-oxidized bacteriochlorophyll dimer P960 in *Blastochloris* (formerly *Rhodopseudomonas*) *viridis* RC by the immediate electron donor, high-potential cytochrome cyt c_{559}, and further electron transfer from the second high-potential cyt c_{556} to oxidized cyt c_{559} account for 15% and 5% of the overall photoresponse amplitude $\Delta\psi$, respectively [34]. The same relative photovoltages and effective dielectric constant values were obtained for the donor sites of the *Rhodospirillum rubrum* and *Rhodobacter sphaeroides* RC [35].

Comparison of the distance vector projections onto the membrane normal with the relative photovoltage amplitudes in PS I and bacterial RC demonstrated that the ε values corresponding to the electron transfer from the native donor proteins to P700 and P960 (or P870 in case of the other bacterial RC species) were close to one another. Note that the electron transport reactions at the donor side of PS I and bacterial RC share the following features of similarity: (i) Gibbs energy difference (ΔG) between Pc/cyt c_6 and P700 is close to ΔG between cyt c_2 and P870; (ii) electron transfer kinetics and proposed reaction mechanisms are very similar.

The main electrogenic step on the acceptor side of bacterial RC is due to the protonation of the double-reduced secondary quinone Q_B [36]. The ε value in this region is ~20 [37], which is about 3 times higher than that in the acceptor region of PS I. The profiles of dielectric constant distribution over electron transfer cofactors in bacterial RC, PS I, and PS II are shown in Fig. 1.

Because similar patterns of distribution of dielectric constant are observed at least in three photosynthetic systems with different structures, it is safe to suggest that such a character of dielectric constant distribution is a general property inherent in photosynthetic charge transfer processes rather than a unique characteristic of specific pigment–protein complexes.

Note also that the thermodynamic and kinetic properties of the terminal acceptors in bacterial RC complexes significantly differ from those in PS I. The redox midpoint potential (E_m) values of the Q_A/Q_A^- and Q_B/Q_B^- redox couples in bacterial RC fall within the range from −50 to +100 mV, whereas the E_m values of F_X, F_A, and F_B in PS I are much more negative (range from −500 to −700 mV). The lifetimes of the electron and proton transfer reactions on the acceptor side of bacterial RC (submillisecond time range) are at least three orders of magnitude lower than those values in the domain of the iron–sulfur clusters in PS I (range of tens to hundreds of nanoseconds). Perhaps, the three-order-of-magnitude difference between the rate constants of charge transfer on the acceptor side of bacterial RC and PS I, and threefold increase in the estimated value of ε reflects hypothetical correlation between the reaction rates and the dielectric properties of the corresponding protein domains between redox cofactors suggested in our earlier works [7–10]. Indeed, the primary processes of electron transfer in photosynthesis are characterized by high rates (reaction time, from pico- to nanoseconds), low value of ε, and large value of the free energy gap ΔG. As the electron goes farther from the primary pair of Chl (or bacteriochlorophyll) molecules, the value of ε gradually increases and reaction rate decreases.

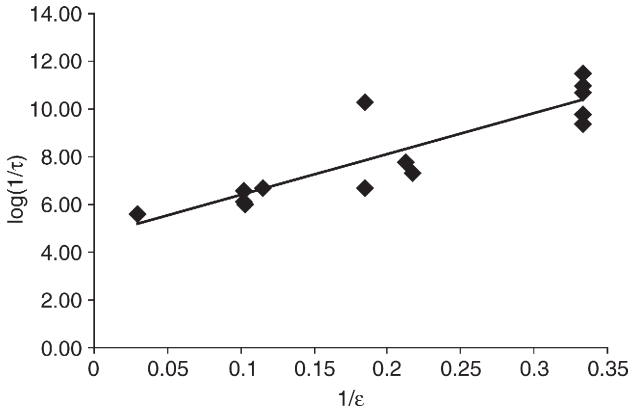

Fig. 2. Dependence of electron transfer rate constant on dielectric permittivity in photosynthetic RC complexes. The experimental points correspond to the donor–acceptor pairs listed in Table 2.

Quantitatively, correlation between dielectric permittivity and electron transfer rate constant is illustrated by empirical data summarized in Fig. 2. Let us consider possible mechanism of the correlation between kinetic and dielectric properties of reaction centers in more detail.

3. Possible mechanism of correlation between kinetic and dielectric properties of reaction centers

Electron transfer reactions in protein complexes occur from a donor (D) to an acceptor (A), which are often held at fixed distance and orientation apart from each other. Two alternative mechanisms of ET could be considered depending on whether the rate of polar environment relaxation is faster or slower than the rate constant of electron tunneling k_0. If the distance between reactants is small enough and k_0 is higher than the rate of medium relaxation (the adiabatic mode), the ET is controlled by the solvent dynamics [38]. In the alternative case, when the rate of solvent relaxation is fast (the nonadiabatic limit), the rate constant of ET could be calculated by the first order time-dependent perturbation theory and, in the high-temperature limit, this approach gives the semiclassical nonadiabatic theory [39]. In ordinary solvents, the medium relaxation is complete in several picoseconds, so the ET reactions which are slower than several picoseconds are usually treated as nonadiabatic ones. In proteins, however, the nonadiabatic ET mechanism might be complicated by relaxation processes in the microsecond time scale, such as slow conformational motion of protein subdomains or proton redistribution at pH-buffering groups. If the driving force of the ET reaction is less or about 0.1 eV, relaxation processes might partially control the ET dynamics [40]. Such relaxation control apparently takes place for slow components of $Q_A \rightarrow Q_B$ ET reaction in bacterial RC from *R. sphaeroides* [41], $P960^+$ reduction by four-heme cytochrome *c* in RC from *B. viridis* [40], and the reduction of photo-oxidized primary donor $P680^+$ by a redox-active tyrosine Y_Z in photosystem II [42,43]. Further we would consider only those ET reactions that occur by the nonadiabatic mechanism.

If the edge-to-edge distance d between donor D and acceptor A exceeds 5–7 Å, the electronic interaction between them is relatively weak and the rate constant for the ET could be estimated by the semiclassical nonadiabatic theory [39]. This theory separates the classical movement of nuclear subsystem from the quantum electron tunneling between D and A and considers the three following stages of the ET reaction: (i) the classical subsystem oscillates stochastically around an equilibrium reactant conformation and reaches randomly the transition state where the energy of reactants matches the energy of products, that requires an activation energy E_a. (ii) In the transition state, the electron tunneling becomes possible with rate constant k_0. (iii) After the electron tunneling, the heavy-atom subsystem relaxes towards an equilibrium product conformation. The criterion of the nonadiabatic mechanism is that the frequency of classical heavy-atom motion around equilibrium and the relaxation towards product state is faster than the rate of electron tunneling k_0. Under this condition, the rate constant of ET k_{ET} is broken up into nuclear and electronic terms:

$$k_{ET} = k_0 \exp(-E_a/k_B T). \quad (1)$$

Here the electronic term k_0 is the rate of electron tunneling (it is proportional to the electronic coupling between redox sites $|H_{AD}|^2$ determined by the protein atomic structure) and the exponential nuclear term relates the activation energy of the transition state to the nuclear reorganization energy λ and the reaction driving force $-\Delta G$:

$$E_a = (\lambda + \Delta G)^2/4\lambda. \quad (2)$$

The values ΔG and geometrical parameters of the electron carriers of bacterial RC, PS I, PS II, and soluble ferredoxin

Table 2
Experimental characteristics of some electron transfer reactions in bacterial photosynthetic reaction center, PS I, PS II, and soluble ferredoxins (Fd)

ET reaction	ε_D	ε_A	ΔG (meV)	d (Å)	a_D (Å)	a_A (Å)	R (Å)	E_a (meV)	τ (s)	Reference for ΔG	Reference for τ
BRC: $c_{556} \rightarrow c_{551}^+$	34	34	300	7.9	5	5	16.5	366	2.2×10^{-6}	[50]	[50]
BRC: $c_{559}^- \rightarrow P960^+$	34	9.8	−130	12.3	5	7	21	40	3×10^{-7}	[34,51]	[34,51]
BRC: $P960^+ \rightarrow B_A$	3	3	−87	5.2	7	5	11.6	0	3.5×10^{-12}	[52]	[52]
BRC: $B_A^- \rightarrow H_A$	3	3	−161	4.9	5	5	10.9	8	1.2×10^{-12}	[52]	[52]
BRC: $H_A^- \rightarrow Q_A$	3	4	−500	9.3	5	4	15	54	2×10^{-10}	[53]	[54]
BRC: $Q_A^- \rightarrow Q_B$ [a]	4	20	−100	13	4	3.5	18	151	2×10^{-5}	[53]	[55]
BRC: $Q_A^- \rightarrow P960^+$	4	3	−580	22.3	4	7	28	78	10^{-1}	[53]	[55]
PS I: $A_0^- \rightarrow A_1$	3	5.4	−300	6.7	5	4	9	2	3×10^{-11}	[56,57]	[58]
PS I: $A_1^- \rightarrow F_X$	5.4	8.7	−100	9	4	3.9	13	211	$2–15\times10^{-8}$	[57,59]	[60]
PS I: $F_X^- \rightarrow F_A$	8.7	6.6	−150	11.5	3.9	3.9	14.1	208	$3–5\times10^{-7}$	[59,61]	[62]
PS I: $F_A^- \rightarrow F_B$	6.6	4.8	50	9.5	3.9	3.9	12	263	$3–5\times10^{-7}$	[61]	[62]
PS II: $Y_Z \rightarrow P680^+$	6.4	3	−90	9	3	7	17	107	$3.5–5\times10^{-8}$ [b]	[63]	[63]
PS II: $^1P680^* \rightarrow B_A$	3	3	0	4.4	7	5	11.3	20	6×10^{-12}	[64]	[65]
PS II: $B_A^- \rightarrow H_A$	3	3	−150	5	5	5	10.7	5	7×10^{-13}	[67]	[66]
PS II: $H_A^- \rightarrow Q_A$	3	4	−340	8.6	5	3.5	13	3	$3–4\times10^{-10}$	[68]	[69]
Fd: $(FeS)_4 \rightarrow (FeS)_4$	6.6	6.6	0	8.5	3.9	3.9	11.7	253	3×10^{-7}	[70]	[70]

[a] This reaction is coupled to a proton transfer, but it is not kinetically limited by the proton transfer.
[b] According to [43], reduction of $P680^+$ by the redox active tyrosine Y_Z is multiphasic. Only the component with largest amplitude was taken into account. The components with lower amplitudes and slower kinetics could be explained by relaxation processes and different conformational states of the system that determine the overall time course. Obviously, the rates of these processes were not simply derived from the Marcus theory.

found in the literature are summarized in Table 2. The reorganization energy of the heavy-atom subsystem λ could be broken up into two terms: the reorganization of redox cofactors themselves and the reorganization of external medium (the inner-sphere and outer-sphere parts λ_{in} and λ_{out}, respectively). In many cases, the molecules of redox cofactors are fairly rigid and the redox transition occurs without considerable conformational changes of the cofactors that leads to negligibly small λ_{in} values, but in the case of $[FeS]_4$ cluster, the λ_{in} value exceeds 0.2 eV [44], and the latter figure was used for $[FeS]_4$ clusters in further calculations. In homogeneous medium λ_{out} could be approximated by the equation:

$$\lambda_{out} = e^2\left(\frac{1}{\varepsilon_o} - \frac{1}{\varepsilon_s}\right)\left(\frac{1}{2a_D} + \frac{1}{2a_A} - \frac{1}{R}\right) \quad (3)$$

where e is the electron charge, ε_o and ε_s are optical and static dielectric constants of the external medium, a_D and a_A are the effective radii of the donor and acceptor, and R is the center-to-center distance between the cofactors. The optical dielectric permittivity of protein is about 2.5; the static dielectric constant might vary in a wide range from 3 to 30 [41,45]. The effective radii of cofactors could be either estimated by their van der Waals volume, or calculated more precisely by numeric integration of the Poisson–Boltzmann equation using special software [46].

The electronic term, k_0, is directly related to the strength of the electronic interaction between the donor and acceptor, which decays exponentially upon increasing the edge-to-edge distance d. Although the secondary and tertiary protein structures might affect the magnitude of the electronic coupling (see, e.g., the discussion in a special issue of *J. Biol. Inorg. Chem.* 2 (1997), and in particular, Ref. [47]), to a first approximation the electronic term could be estimated by the empirical Moser–Dutton expression that describes a simple exponential decay of tunneling rate with the distance d [48]:

$$k_0 = 10^{13-0.6(d-3.6)}(s^{-1}). \quad (4)$$

Quantitatively, Eqs. (1), (2), and (3) describe the dependence of the rate constant k_{ET} on the local dielectric permittivity of the protein ε_s in the vicinity of cofactors completed by the geometry factor specified by Eq. (4). To compare the ET reactions occurring at different distances, it is worthwhile excluding the dependence of the ET rate on the distance and to use a corrected rate constant

$$k^0_{ET} = k_{ET}\cdot 10^{0.6(d-3.6)}. \quad (5)$$

The corrected rate constant of a given ET reaction is an ideal rate at very strong electronic coupling of reactants (if the reactants are in direct contact). The usage of distance-excluded rate constant k^0_{ET} is complementary to the usage of free-energy-optimized ET rate by Moser and Dutton who excluded the nuclear term ($-\Delta G_{opt}=\lambda$) and quantified the effect of distance on the ET rate [48].

As the local dielectric permittivity might be significantly different in the vicinity of donor and acceptor, it seems reasonable to plot the dependence of the distance-excluded rate constant k^0_{ET} on the activation energy calculated from Eq. (2) using the following approximation for the reorganization energy [49]:

$$\lambda = \lambda_{in} + \frac{e^2}{2a_D}\left(\frac{1}{\varepsilon_0} - \frac{1}{\varepsilon_D}\right) + \frac{e^2}{2a_A}\left(\frac{1}{\varepsilon_0} - \frac{1}{\varepsilon_A}\right) - \frac{e^2}{R}\left(\frac{1}{\varepsilon_0} - \frac{\varepsilon_D + \varepsilon_A}{2\varepsilon_A\varepsilon_D}\right). \quad (6)$$

This equation takes into account dielectric heterogeneity of protein by using different values of static dielectric permittivity ε_D and ε_A in the vicinity of donor and acceptor, respectively.

Fig. 3 shows the dependence of the distance-excluded rate constant on the activation energy calculated from Eqs. (2) and (6) using experimental results and data available from the literature and summarized in Table 2. The solid line shows the ideal dependence at direct contact between cofactors (d=3.6 Å, $k_0=10^{13}$ s^{-1}), whereas each experimental point corresponds to individual donor–acceptor pair with specific geometric parameters (a_D, a_A, R, d), dielectric properties (ε_D and ε_A), and driving force value ($-\Delta G$).

The correlation of experimental points obtained for various donor–acceptor pairs in different pigment–protein complexes of three photosynthetic systems (RC of purple bacteria and PS I and PS II of cyanobacteria) and soluble ferredoxin with the ideal theoretical dependence demonstrates that:

(1) All ET reactions considered in this work follow the nonadiabatic mechanism and can be semiquantitatively described in terms of the Marcus theory using the Moser–Dutton empirical rule for electronic coupling term.
(2) The local dielectric permittivity of membrane proteins inferred from the electrometric experiments could be used

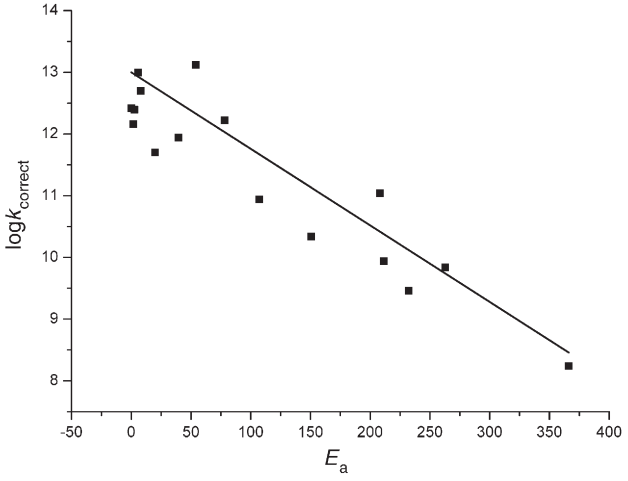

Fig. 3. Comparison of calculated (solid line) with experimental (squares) distance-excluded rate constants k^0_{ET} for various electron transfer reactions in bacterial photosynthetic reaction centers, photosystems I and II and soluble ferredoxin. Measured rates, ΔG, geometric and dielectric parameters are taken from Table 2, reorganization energy λ and activation energy E_a are calculated from Eqs. (2) and (6), respectively.

for calculation of the ET reorganization energy by methods of continuum electrostatics.

(3) Simple models of macroscopic electrostatics could be successfully applied to the ET reactions in membrane proteins with resolved atomic structure predicting the rate constant with the accuracy of less than one order of magnitude.

Further research into the possible mechanism of correlation between these parameters is a subject of our planned experimental and theoretical study.

Acknowledgments

The authors are grateful to Prof. L.I. Krishtalik for the valuable discussions and Dr. R.H. Lozier for critical reading of the manuscript.

This study was supported by Grants from Russian Foundation for Basic Research 06-04-48672, 05-04-48557 and 06-04-48719 and from Russian Federal Agency for Science and Innovation.

References

[1] L.A. Drachev, A.A. Jasaitis, A.D. Kaulen, A.A. Kondrashin, E.A. Liberman, I.B. Nemecek, S.A. Ostroumov, A.Yu. Semenov, V.P. Skulachev, Direct measurement of electric current generation by cytochrome oxidase, H^+-ATPase and bacteriorhodopsin, Nature 249 (1974) 321–324.

[2] L.A. Drachev, A.D. Kaulen, L.V. Khitrina, V.P. Skulachev, Fast stages of photoelectric processes in biological membranes: I. Bacteriorhodopsin, Eur. J. Biochem. 117 (1981) 461–470.

[3] L.A. Drachev, A.Yu. Semenov, V.P. Skulachev, I.A. Smirnova, S.K. Chamorovsky, A.A. Kononenko, A.B. Rubin, N.Ya. Uspenskaya, Fast stages of photoelectric processes in biological membranes: III. Bacterial photosynthetic redox system, Eur. J. Biochem. 117 (1981) 483–489.

[4] M.D. Mamedov, R.M. Gadjieva, K.N. Gourovskaya, L.A. Drachev, A.Yu. Semenov, Electrogenicity at the donor/acceptor sides of cyanobacterial photosystem I, J. Bioenerg. Biomembr. 28 (1996) 517–522.

[5] I.R. Vassiliev, Y.-S. Jung, M.D. Mamedov, A.Yu. Semenov, J.H. Golbeck, Near-IR absorbance changes and electrogenic reactions in the microsecond-to-second time domain in photosystem I, Biophysical. J. 72 (1997) 301–315.

[6] M.D. Mamedov, E.R. Lovyagina, M.I. Verkhovsky, A.Yu. Semenov, D.A. Cherepanov, V.P. Shinkarev, Generation of the electrical potential difference by photosystem II from thermophilic cyanobacteria, Biochemistry (Moscow) 59 (1995) 327–341.

[7] A.Yu. Semenov, M.D. Mamedov, S.K. Chamorovsky, Photoelectric studies of the transmembrane charge transfer reactions in photosystem I pigment–protein complexes, FEBS Lett. 553 (2003) 223–228.

[8] A.Yu. Semenov, S.K. Chamorovsky, M.D. Mamedov, Electrogenic reactions in photosystem I complexes, Biofizika 49 (2004) 227–238.

[9] A.Yu. Semenov, M.D. Mamedov, S.K. Chamorovsky, Electrogenic reactions associated with electron transfer in photosystem I, in: J.H. Golbeck (Ed.), The Light-driven Plastocyanin, Springer, 2006, pp. 319–338.

[10] C.S. Chamorovsky, S.K. Chamorovsky, A.Yu. Semenov, Dielectric and photoelectric properties of photosynthetic reaction centers, Biochemistry (Moscow) 70 (2005) 315–322.

[11] P. Jordan, P. Fromme, O. Klukas, H.T. Witt, W. Saenger, N. Krauss, Three-dimensional structure of cyanobacterial photosystem I at 2.5 Å resolution, Nature 411 (2001) 909–917.

[12] P. Fromme, W.D. Schubert, N. Krauss, Structure of photosystem I: suggestions on the docking sites for plastocyanin, ferredoxin and the coordination of P700, Biochim. Biophys. Acta 1187 (1994) 99–105.

[13] E. Myshkin, N.B. Leontis, S. Bullerjahn, Computational simulation of the docking of *Prochlorothrix hollandica* plastocyanin to photosystem I: modeling the electron transfer complex, Biophys. J. 82 (2002) 3305–3313.

[14] B. Hecks, J. Breton, W. Leibl, K. Wulf, H.-W. Trissl, Primary charge separation in photosystem I: a two-step electrogenic charge separation connected with $P700^+A_0^-$ and $P700_+A_1^-$ formation, Biochemistry 33 (1994) 8619–8624.

[15] W. Leibl, B. Toupance, J. Breton, Photoelectric characterization of forward electron transfer to iron–sulfur centers in photosystem I, Biochemistry 34 (1995) 10237–10244.

[16] A. Diaz-Quintana, W. Leibl, H. Bottin, P. Setif, Electron transfer in photosystem I reaction centers follows a linear pathway in which iron–sulfur cluster FB is the immediate electron donor to soluble ferredoxin, Biochemistry 37 (1998) 3429–3439.

[17] M.D. Mamedov, K.N. Gourovskaya, I.R. Vassiliev, J.H. Golbeck, A.Yu. Semenov, Electrogenicity accompanies photoreduction of the iron–sulfur clusters FA and FB in photosystem I, FEBS Lett. 431 (1998) 219–223.

[18] M.D. Mamedov, A.A. Mamedova, S.K. Chamorovsky, A.Yu. Semenov, Electrogenic reduction of the primary electron donor P700 by plastocyanin in photosystem I complexes, FEBS Lett. 500 (2001) 172–176.

[19] A.A. Mamedova, M.D. Mamedov, K.N. Gourovskaya, I.R. Vassiliev, J.H. Golbeck, A.Yu. Semenov, Electrometrical study of electron transfer from the terminal FA/FB iron–sulfur clusters to external acceptors in photosystem I, FEBS Lett. 462 (1999) 421–424.

[20] M.L. Antonkine, P. Jordan, P. Fromme, N. Krauss, J.H. Golbeck, D. Stehlik, Assembly of protein subunits in stromal ridge of photosystem I. Structural changes between unbound and sequentially PS I-bound polypeptides and correlated changes of magnetic properties of terminal iron sulfur centers, J. Mol. Biol. 327 (2003) 671–697.

[21] A. Zouni, H.-T. Witt, J. Kern, P. Fromme, N. Krauss, W. Saenger, P. Orth, Crystal structure of photosystem II from *Synechococcus elongatus* at 3.8 Å resolution, Nature 409 (2001) 739–743.

[22] N. Kamiya, J.-R. Shen, Crystal structure of oxygen-evolving photosystem II from *Thermosynechococcus valcanus* at 3.7 Å resolution, Proc. Natl. Acad. Sci. U. S. A. 100 (2003) 98–103.

[23] K.N. Ferreira, T.M. Iverson, K. Maghlaoui, J. Barber, S. Iwata, Architecture of the photosynthetic oxygen-evolving centre, Science 303 (2004) 1831–1838.

[24] B. Loll, J. Kern, W. Saenger, A. Zouni, J. Biesiadka, Towards complete cofactor arrangement in the 3.0 Å resolution structure of photosystem II, Nature 438 (2005) 1040–1044.

[25] H.-W. Trissl, W. Leibl, Primary charge separation in photosystem II involves two electrogenic steps, FEBS Lett. 244 (1989) 85–88.

[26] W. Leibl, J. Breton, J. Deprez, H.-W. Trissl, Photoelectric study on the kinetics of trapping and charge stabilization in oriented PS II membranes, Photosynth. Res. 22 (1989) 257–275.

[27] A. Pokorny, K. Wulf, H.-W. Trissl, An electrogenic reaction associated with the re-reduction of P680 by Tyr Z in Photosystem II, Biochim. Biophys. Acta 1184 (1994) 65–70.

[28] M. Haumann, A. Mulkidjanian, W. Junge, Electrogenicity of electron and proton transfer at the oxidizing side of photosystem II, Biochemistry 36 (1997) 9304–9315.

[29] M.D. Mamedov, O.E. Beshta, K.N. Gourovskaya, A.A. Mamedova, K.D. Neverov, V.D. Samuilov, A.Yu. Semenov, Photoelectric responses of oxygen-evolving complexes of photosystem II, Biochemistry (Moscow) 64 (1999) 504–509.

[30] M.D. Mamedov, O.E. Beshta, V.D. Samuilov, A.Yu. Semenov, Electrogenicity at the secondary quinone acceptor site of cyanobacterial photosystem II, FEBS Lett. 350 (1994) 96–98.

[31] F. Hook, P. Brzezinski, Light-induced voltage changes associated with electron and proton transfer in photosystem II core complexes reconstituted in phospholipid monolayers, Biophys. J. 66 (1994) 2066–2072.

[32] F. Rappaport, M. Guergova-Kuras, P.J. Nixon, B.A. Diner, J. Laverhne, Kinetics and pathways of charge recombination in photosystem II, Biochemistry 41 (2002) 8518–8527.

[33] M.D. Mamedov, A.A. Tyunyatkina, A.Yu. Semenov, Electrogenic

protonation of the secondary quinone acceptor Q_B in spinach photosystem II complexes incorporated into lipid vesicles, Biochemistry (Moscow) 70 (2005) 1348–1353.
[34] S.M. Dracheva, L.A. Drachev, A.A. Konstantinov, A.Yu. Semenov, V.P. Skulachev, A.M. Arutyunian, V.A. Shuvalov, S.M. Zaberezhnaya, Electrogenic steps in the redox reactions catalyzed by photosynthetic reaction-centre complex from *Rhodopseudomonas viridis*, Eur. J. Biochem. 171 (1988) 253–264.
[35] A.Yu. Semenov, Electrogenic reactions in photosynthetic reaction centers of purple bacteria, in: V.P. Skulachev (Ed.), Electrogenic Reactions in Photosynthetic Reaction Centres of Purple Bacteria, Soviet scientific reviews/section D, 10, Harwood Academic Publishers, 1991, pp. 45–75.
[36] O.P. Kaminskaya, L.A. Drachev, A.A. Konstantinov, A.Yu. Semenov, V.P. Skulachev, Electrogenic reduction of the secondary quinone acceptor in chromatophores of *Rhodospirillum rubrum*: rapid kinetics measurements, FEBS Lett. 202 (1986) 224–228.
[37] V.P. Shinkarev, L.A. Drachev, M.D. Mamedov, A.Ya. Mulkidjanian, A.Yu. Semenov, M.I. Verkhovsky, Effect of pH and surface potential on the rate of electric potential generation due to proton uptake by secondary quinone acceptor of reaction centers in *Rhodobacter sphaeroides* chromatophores, Biochim. Biophys. Acta 1144 (1993) 285–294.
[38] R.R. Dogonadze, Z.D. Urushadze, Semiclassical method of calculation of chemical reactions proceeding in polar liquids, J. Electroanal. Chem. 32 (1971) 234–245.
[39] R.A. Marcus, N. Sutin, Electron transfer in chemistry and biology, Biochim. Biophys. Acta 811 (1985) 265–322.
[40] D.A. Cherepanov, L.I. Krishtalik, A.Y. Mulkidjanian, Photosynthetic electron transfer controlled by protein relaxation: analysis by Langevin stochastic approach, Biophys. J. 80 (2001) 1033–1049.
[41] D.A. Cherepanov, S.I. Bibikov, M.V. Bibikova, D.A. Bloch, L.A. Drachev, O.A. Gopta, D. Oesterhelt, A.Y. Semenov, A.Y. Mulkidjanian, Reduction and protonation of the secondary quinone acceptor of *Rhodobacter sphaeroides* photosynthetic reaction center: kinetic model based on a comparison of wild-type chromatophores with mutants carrying Arg→Ile substitution at sites 207 and 217 in the L-subunit, Biochim. Biophys. Acta 1459 (2000) 10–34.
[42] D.A. Cherepanov, W. Drevenstedt, L.I. Krishtalik, A. Mulkidjanian, W. Junge, Protein relaxation and kinetics of P_{680} reduction in photosystem II, in: G. Garab (Ed.), Photosynthesis: Mechanism and Effects, Kluwer Acad. Publishers, The Netherlands, 1998, pp. 1073–1076.
[43] P. Kuehn, H.-J. Eckert, H.J. Eichlerb, G. Renger, Analysis of the P_{680} reduction pattern and its temperature dependence in oxygen-evolving PS II core complexes from thermophilic cyanobacteria and higher plants, Phys. Chem. Chem. Phys. 6 (2004) 4838–4843.
[44] E. Sigfridsson, M.H.M. Olsson, U. Ryde, A comparison of the inner-sphere reorganisation energies of cytochromes, iron–sulphur clusters, and blue copper proteins, J. Phys. Chem., B 105 (2001) 5546–5552.
[45] M.A. Steffen, K. Lao, S.G. Boxer, Dielectric Asymmetry in the Photosynthetic Reaction Center, Science 264 (1994) 810–816.
[46] W. Rocchia, S. Sridharan, A. Nicholls, E. Alexov, A. Chiabrera, B. Honig, Rapid grid-based construction of the molecular surface for both molecules and geometric objects: applications to the finite difference Poisson–Boltzmann method, J. Comp. Chem. 23 (2002) 128–137.
[47] J.R. Winkler, H.B. Gray, Electron tunneling in proteins: role of the intervening medium, J. Biol. Inorg. Chem. 2 (1997) 399–404.
[48] C.C. Moser, J.M. Keske, K. Warncke, R.S. Farid, P.L. Dutton, Nature of biological electron transfer, Nature 355 (1992) 796–802.
[49] R.A. Marcus, Reorganization free energy for electron transfers at liquid–liquid and dielectric semiconductor–liquid interfaces, J. Phys. Chem. 94 (1990) 1050–1055.
[50] I.-P. Chen, P. Mathis, J. Koepke, H. Michel, Uphill electron transfer in the tetraheme cytochrome subunit of the *Rhodopseudomonas viridis* photosynthetic reaction center: evidence from site-directed mutagenesis, Biochemistry 39 (2000) 3592–3602.
[51] S.M. Dracheva, L.A. Drachev, S.M. Zaberezhnaya, A.A. Konstantinov, A. Yu. Semenov, V.P. Skulachev, Spectral, redox and kinetic characteristics of high-potential cytochrome *c* hemes in *Rhodopseudomonas viridis* reaction center, FEBS Lett. 205 (1986) 41–46.
[52] C. Lauterwasser, U. Finkele, H. Scheer, W. Zinth, Temperature dependence of the primary electron transfer in photosynthetic reaction centers from *Rhodobacter sphaeroides*, Chem. Phys. Lett. 183 (1991) 471–477.
[53] R.C. Prince, P.L. Dutton, Protonation and reducing potential of the primary electron acceptor, in: R.K. Clayton, W.R. Systrom (Eds.), The Photosynthetic Bacteria, Plenum Press, New York, 1978, pp. 439–453.
[54] W. Parson, Electron transfer in reaction centers, in: H. Scheer (Ed.), Chlorophylls, CRC Press, Boca Raton, FL, 1991, pp. 1153–1180.
[55] P. Mathis, I. Sinning, H. Michel, Kinetics of electron transfer from the primary to the secondary quinone in *Rhodopseudomonas viridis*, Biochim. Biophys. Acta 1098 (1992) 151–158.
[56] V.A. Shuvalov, Photosynthetic Primary Charge Separation of Light Energy, Nauka, Moscow, 1990.
[57] M.H. Vos, H.J. van Gorkom, Thermodynamics of electron transport in photosystem I studied by electric field-stimulated charge recombination, Biochim. Biophys. Acta 934 (1988) 293–302.
[58] K. Brettel, M.H. Vos, Spectroscopic resolution of the picosecond reduction kinetics of the secondary electron acceptor A1 in photosystem I, FEBS Lett. 447 (1999) 315–317.
[59] S.K. Chamorovsky, R. Cammack, Direct determination of the midpoint potential of the acceptor X in chloroplast Photosystem I by electrochemical reduction and ESR spectroscopy, Photobiochem. Photobiophys. 4 (1982) 195–200.
[60] P. Setif, K. Brettel, Forward electron transfer from phylloquinone A1 to iron–sulfur centers in spinach photosystem I, Biochemistry 32 (1993) 7846–7854.
[61] J.H. Golbeck, Photosystem I in cyanobacteria, in: D.A. Bryant (Ed.), The Molecular Biology of Cyanobacteria, Kluwer Acad. Publishers, The Netherlands, 1994, pp. 179–220.
[62] K. Brettel, W. Leibl, Electron transfer in photosystem I, Biochim. Biophys. Acta 1507 (2001) 100–114.
[63] J.G. Metz, P.J. Nixon, M. Rögner, G.W. Brudvig, B.A. Diner, Directed alteration of the D1 polypeptide of photosystem II: evidence that tyrosine-161 is the redox component, Z, connecting the oxygen-evolving complex to the primary electron donor, P680, Biochemistry 28 (1989) 6960–6969.
[64] H.-J. Eckert, G. Renger, Temperature dependence of $P680^+$ reduction in O_2-evolving PS II membrane fragments at different redox states S_i of the water oxidizing system, FEBS Lett. 236 (1988) 425–431.
[65] B. Meyer, E. Schlodder, J.P. Dekker, H.T. Witt, O_2 evolution and Chl aII+ (P680+) nanosecond reduction kinetics in single flashes as a function of pH, Biochim. Biophys. Acta 974 (1989) 36–43.
[66] M.L. Groot, N.P. Pawlowicz, L.J.G.W. van Wilderen, J. Breton, I.H.M. van Stokkum, R. van Grondelle, Initial electron donor and acceptor in isolated Photosystem II reaction centers identified with femtosecond mid-IR spectroscopy, Proc. Natl. Acad. Sci. U. S. A. 102 (2005) 13087–13092.
[67] C.C. Moser, C.C. Page, P.L. Dutton, Tunneling in PSII, Photochem. Photobiol. Sci. 4 (2005) 933–939.
[68] A. Krieger, A.W. Rutherford, G.N. Johnson, On the determination of redox midpoint potential of the primary quinone electron acceptor, QA, in photosystem II, Biochim. Biophys. Acta 1229 (1995) 193–201.
[69] J. Bernarding, H.-J. Eckert, H.J. Eichler, A. Napiwotzki, G. Renger, Kinetic studies on the stabilization of the primary radical pair P680+ Pheo− in different photosystem II preparations from higher plants, Photochem. Photobiol. 59 (1994) 566–573.
[70] P. Kyritsis, G. Huber, I. Quinkal, J. Gaillard, J.-M. Moulis, Intramolecular electron transfer between [4Fe-4S] clusters studied by proton magnetic resonance spectroscopy, Biochemistry 36 (1997) 7839–7846.